

TWO-MODES CYCLIC BIOSIGNAL CLUSTERING BASED ON TIME SERIES ANALYSIS

Neuza Nunes, Tiago Araújo
Physics Department, FCT-UNL, Lisbon, Portugal
neuzanunes@gmail.com, tiago_sergio87@hotmail.com

Hugo Gamboa
Physics Department, FCT-UNL, Lisbon, Portugal
PLUX – Wireless Biosignals, Lisbon, Portugal
h.gamboa@fct.unl.pt, hgamboa@plux.info

Keywords: Biosignals, waves, unsupervised learning, clustering, data mining, signal-processing.

Abstract: In this paper we introduce an unsupervised learning algorithm which distinguishes two different modes in a cyclic signal. We also present the concept of “*mean wave*” which averages all signal waves aligned in a notable point (n^{th} zero derivative). With that information the signal’s morphology is captured. The clustering mechanism is based on the information collected with the *mean wave* approach using a k-means algorithm. The algorithm produced is signal-independent, and therefore can be applied to any type of signal providing it is a cyclic signal that has no major changes in the fundamental frequency. To test the effectiveness of the proposed method, we acquired several biosignals (accelerometry, electromyography and blood volume pressure signals) in the context tasks performed by the subjects with two distinct modes in each. The algorithm successfully separates the two modes with 99.2% of efficiency. The fact that this approach doesn’t require any prior information and the preliminary good classification performance makes this algorithm a powerful tool for biosignals analysis and classification.

1 INTRODUCTION

Human-activity tracking techniques focus on direct observation of people and their behavior. This could be done, as an example, with cameras (Jezekiel Ben-Arie, 2002), accelerometers to track human motion (Jonghun Baek et al., 2004), or contact switches to compute facial expressions with the electromyography patterns (Joshua R. Smith, 2005) (Alan J. Fridlund, 2007).

In this work we acquired several cyclic biosignals – such as accelerometry (ACC), electromyography (EMG) and blood volume pressure (BVP) signals – from subjects performing some context tasks, and we’ve developed an unsupervised learning algorithm which is capable to distinguish two different modes in the same acquired signal.

The developed algorithm follows an unsupervised learning approach, as it doesn’t require any prior information (Zoubin Ghahramani, 2004).

We use the k-means cluster algorithm due to its efficiency and effectiveness (Xindong Wu, 2007).

As a clustering method, our algorithm is signal-independent and doesn’t use specific information about the signals. Although our algorithm is signal-independent, the signals used must be cyclic signals, with only two distinctive modes and a small variation of fundamental frequency between those modes.

Warren Liao (2005) presents a survey on time series data clustering, exposing past researches on the subject. He organizes the works in three groups: whether they work directly with the raw data, indirectly with features extracted or indirectly with models built from the raw data. We created a different algorithm as we intended to work with single signals with different modes or activities in it, and the previous studies uses various signals each one distinct with only one mode or activity.

A more resemble approach, as the clustering is based on the similarity of wave shapes presented in a single time series data, is the work of Dr. Rodrigo

Quiroga (2007) with spike sorting. However, as the neuron activity is not periodic, the spikes are detected with a threshold and the clustering procedure uses features extracted from those parts of the signal.

We present the concept of “*mean wave*” which averages all signal waves aligned in a notable point, that we call triggering point, such as maximum, minimum, zero or inflexion point. Our algorithm automatically separates each signal’s cycle and computes the *mean wave* using an alignment on the triggering point of each cycle. With that information the signal’s morphology is captured. Our clustering algorithm uses the signal’s cycles information gathered from the *mean wave* approach to separates the two modes cycles of the entire signal.

As our *mean wave* approach effectively captures the morphology of a signal, can be useful in several areas – as a clustering basis or just for a simple signal analysis.

In the following section the signal acquisition methodology is presented. In section 3 we expose the signal processing detailing all algorithms steps. Finally in sections 4 and 5 we detail and discuss our results and algorithm performance, concluding the work.

2 METHODS

2.1 Acquisition system and sensors

To acquire the biosignals necessary to this study we used a surface electromyography (EMG) sensor, emgPLUX, a triaxial accelerometer (ACC), xyzPLUX, and a finger blood volume pressure (BVP) sensor, bvpPLUX (bioPLUX Research Manual, 2010).

For the signal’s analog to digital conversion and bluetooth transmission to the computer we used a wireless signal acquisition system, bioPLUX research, which has 12 bit ADC and a sampling frequency of 1000 Hz (bioPLUX Research Manual, 2010). In the acquisitions with accelerometers just the axis with inferior-superior direction was connected to the bioPLUX.

2.2 Data acquisition and data format

Several tasks were designed and executed in order to acquire signals that had two distinctive modes.

We conceived a synthetic digital signal and collected signals from four different activities scenarios with the accelerometer sensor, and one for each EMG and BVP sensors.

2.2.1 Synthetic signal

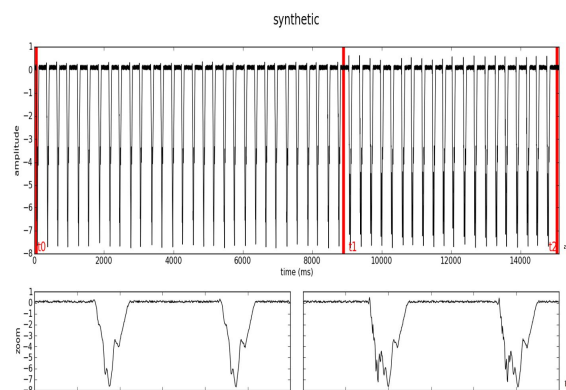


Figure 1 a): Synthetic signal with identical waves from t_0 to t_1 and from t_1 to t_2 ; b): corresponding zoomed waves.

To test our algorithm, a synthetic wave (Figure 1) created using a low-pass filtered random walk (of 100 samples), with a moving average smoothing window of 10% of signal’s length, and multiplied by a hanning window, was repeated 30 times, so all the cycles were identical. After a small break on the signal the wave was repeated 20 more times, with an identical small change of 40 samples in all waves, creating a second mode.

2.2.2 Walking and running (ACC)

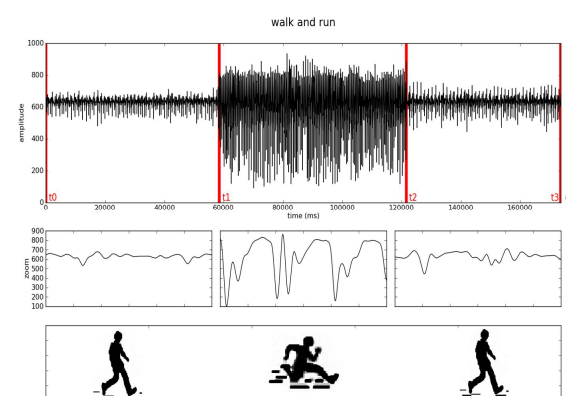


Figure 2 a): Acceleration signal of walking (t_0 to t_1 and t_2 to t_3) and running (t_1 to t_2); b): corresponding zoomed waves; c): tasks performed.

With an accelerometer located at the right hip and oriented so the y axis of the accelerometer (the only connected to the bioPLUX) was pointing upward, the subjects performed a task of walking and running non-stop (on a large circle drawn on the floor).

The subjects walked for about 1 minute at a slow speed, then spent 1 minute running, and ended with 1 minute walking again. The signal acquired is represented in figure 2.

2.2.3 Running and jumping (ACC)

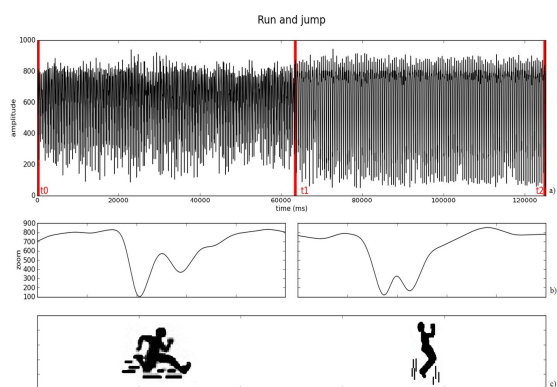


Figure 3 a): Acceleration signal of running (t0 to t1) and jumping (t1 to t2); b): corresponding zoomed waves; c): tasks performed.

With an accelerometer located at the right hip and oriented so the y axis of the accelerometer (the only connected to the bioPLUX) was pointing upward, the subjects performed a task of running non-stop (on a large circle drawn on the floor) and jumping also continuously but at the same place.

The subjects spent 1 minute running, followed by 1 minute jumping. The signal acquired is represented in figure 3.

2.2.4 Jumping with and without impulsion (ACC)

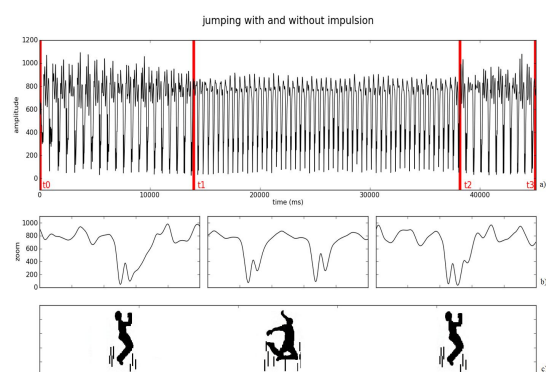


Figure 4 a): Acceleration signal of normal jumps (t0 to t1 and t2 to t3) and jumps with boost (t1 to t2); b): corresponding zoomed waves; c): tasks performed.

In this task, the following procedure was executed: 14 seconds of “normal” jumping (small jumps without a big impulsion), 24 seconds of jumping with some boost and again 7 seconds of normal jumping.

The subjects used an accelerometer located at the right hip and oriented so the y axis of the accelerometer (the only connected to the bioPLUX) was pointing upward. The signal acquired is represented in figure 4.

2.2.5 Skiing (ACC)

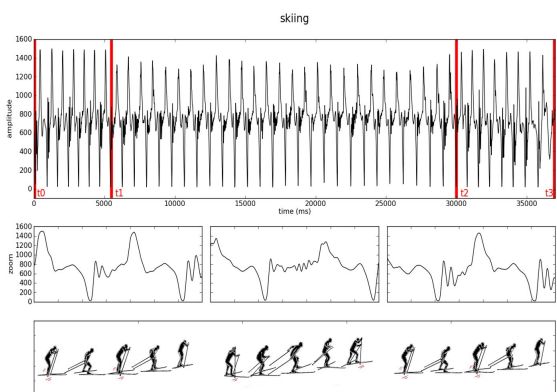


Figure 5 a): Acceleration signal of skiing with V2 technique (t0 to t1 and t2 to t3) and skiing with V1 technique (t1 to t2); b): corresponding zoomed waves; c): tasks performed.

Figure 5 shows the acceleration signal of an accelerometer attached to the ski pole, below the handgrip, used by the subject when skiing.

In the 37 seconds of the signal the subject performed two different techniques, called V1 and V2. V1 skate is an asymmetrical uphill technique

involving one poling action over every second leg stroke. V2 skate is used for moderate uphill slopes and on level terrain, involving one poling action for each leg stroke. (Erik Andersson, 2010)

The first 7 cycles of the signal (about 5 seconds) were produced through a V2 technique, the next 27 cycles (about 25 seconds) a V1 technique and the final 8 cycles the technique was V2 again.

2.2.6 Elevation and squat of the legs (EMG)

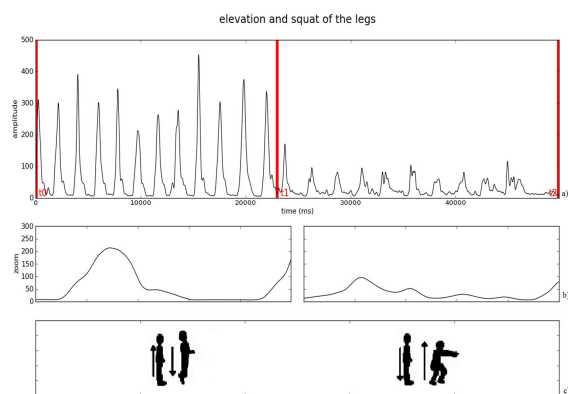


Figure 6 a): EMG signal of the gastrocnemius muscle's contraction through the elevation (t0 to t1) and squat (t1 to t2) of the inferior members; b): corresponding zoomed waves; c): tasks performed.

The subject was standing straight with both feet completely on the ground and was asked to performed 12 elevations of the legs - getting on the tiptoes and back with both feet completely on the ground - followed by 11 squats - bending the knees and back standing straight - (Figure 6). The EMG data were collected using bipolar electrodes at the gastrocnemius muscles of the right leg.

2.2.7 Normal (at rest) and high beat (after exercise) signal (BVP)

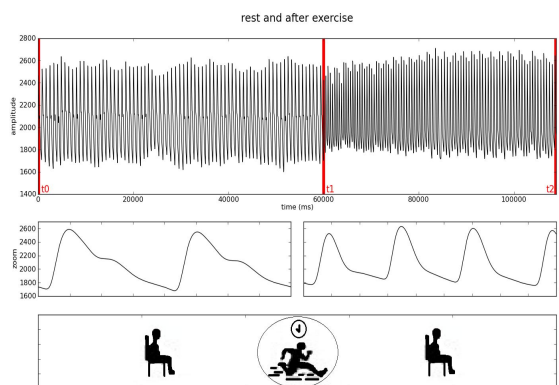


Figure 7 a): BVP signal with the subject at rest (t0 to t1) and after exercise (t1 to t2); b): corresponding zoomed waves; c): tasks performed.

The subjects were instrumented with a BVP sensor on the fourth finger of the left hand and were seating with his left forearm resting on a platform.

We've made one acquisition with the subject at rest. The subjects performed intensive exercise that was not collected to avoid undesirable artefacts due to movement. After the exercise, we acquired another BVP signal.

For the purpose of this study we used both signals (at rest and after exercise) in the same file, cutting a part of each signal and concatenating them offline. The resulting signal is represented in figure 7.

All the signals referenced above are available at OpenSignals (Opensignals.net website, 2010).

3 SIGNAL PROCESSING

The collected data was processed offline using Python with the numpy (T. Oliphant, 2006) and scipy (T. Oliphant, 2007) packages.

Signal processing algorithms were developed for automatic detection of a *mean wave* representative of the signal's behavior and the k-means algorithm was used to cluster the signals. The main idea of this algorithm is to define a loop with k centroids far away from each other, take each point belonging to a given data set and associate it to the nearest centroid. Repeating the loop, the centroids position will change because they are re-calculated as barycenters of the clusters result, and after several iterations the position will stabilize and we achieved the final clusters (D enis Martins, 2008).

Figure 8 describes the method used to process the signals. All biosignals were submitted to a

signal-specific pre-processing phase and then to a generic signal-independent phase (composed with a *mean wave* and clustering procedure) which was applied to all the signals of this study.

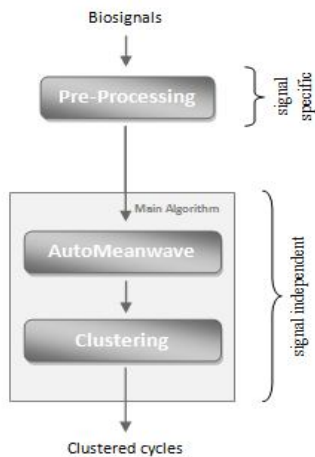


Figure 8: Signal’s processing procedure schematics.

For the pre-processing phase, the acceleration signals were low-pass filtered using a smoothing filter with a moving average window of 50 points. The BVP signal was also low-pass filtered with the same moving average window as the acceleration signals. Random noise with 1/5 of original amplitude was added to the synthetic signal. The EMG signal was centered at y axis zero, by subtracting its mean value, and then rectified. Then we applied the smoothing filter with a moving average window of 300 points.

In the next sections the generic processing procedure will be described.

3.1 Mean wave

Algorithm 1	autoMeanwave
Input:	Signal, sampling frequency, trigger mode.
Output:	Fundamental frequency, window size, events.

The autoMeanwave algorithm is the base function to identify the individual waves. After running this algorithm we will have the *mean wave* computed with the individual wave’s information.

This algorithm receives, by input, a signal, its sampling frequency and a trigger mode (this one can be omitted and the algorithm will use the maximum point as default).

As we’re working with cyclic signals, the first step of the automatic *mean wave* algorithm is the detection of the signal’s fundamental frequency. For that we use the fundamentalFrequency algorithm. With the result we compute the window size value and randomly selected a part of the signal with the same number of samples as the window size. With that signal’s part and the original signal itself we run sumvolve algorithm to get the signal events (series of points that we consider the center of each cycle).

After this we have all the information necessary to compute the *mean wave*, which we do in the computeMeanwave algorithm.

Next we will describe minutely the sub-algorithms referenced above.

Algorithm 2	fundamentalFrequency
Input:	Signal, sampling frequency.
Output:	Fundamental frequency.

In the fundamentalFrequency function, we smoothed the result of the original signal’s fast fourier transform with a moving average window of 5% of the signal’s length. We assumed the frequency value of the first big peak located at the smoothed FFT signal as the fundamental frequency of the original signal.

With the fundamental frequency value we could compute the sampling size of a signal’s cycle. We call that value “window size”, with a 20% margin:

$$\text{winsize} = (f_s / f_0) * 1.2 \quad (1)$$

Being f_s the sampling frequency and f_0 the fundamental frequency. We open the window 20% to use some more samples than a cycle.

Although there are more robust methods to determine the fundamental frequency of a signal, this approach is adequate for our work as the purpose was to have a close idea of the size of a cycle. We actually use more than one exact cycle as we use a margin of 20%, opening the window calculated with the fundamental frequency. Notice that further on we use a correlation function to detect meaningful events on a cycle, so the fundamental frequency is just used as a preliminary estimation to support others algorithms.

Algorithm 3	sumvolve
Input:	Two signals
Output:	Distance values.

This algorithm works as a correlation function. Sliding the smaller window part of the signal (given by argument) through the original signal, one sample at a time, this algorithm compares the distance of the two windows. We used the mean square error as the distance function:

$$f(x) = \sqrt{\frac{\sum_{n=1}^{W_2} (W_1(n-x) - W_2(n))^2}{n}} \quad (2)$$

The result of this algorithm is a signal composed with distance values. That distance values shows the difference between each sliding winsize cycle and the window selected at the first place.

After, we found all the minimum peaks of the resulted correlation signal. Those peaks will be our events.

Algorithm 4	computeMeanwave
Input:	Signal, events, window size.
Output:	Mean wave and standard deviation error wave.

With the events and the window size, we cut the signal into periods that we assume as our signal cycles:

$$\text{cycle} = \text{signal}[\text{event} - \text{winsize}/2 : \text{event} + \text{winsize}/2] \quad (3)$$

This way, based on all cycles, we could compute the mean value to each cycle sample, and compose a *mean wave*. The *standard deviation error wave* is computed with the same principle, calculating the standard deviation error instead of the mean value. For a better visualization of the results, we computed an error area with the *standard deviation error wave* obtained. For that, we added and subtracted one *standard deviation error wave* to the *mean wave*, getting a superior and inferior wave, to graphically present the error area (66% of the error). This is shown in the results section.

After the results shown above, a final adjustment was made: the alignment of every signal's cycles. The position of the *mean wave*'s minimum point

was detected, and that become our trigger point. The minimum position was chosen as the trigger position - we could use the maximum (of the signal or the derivative), or the zero crossings, for example.

With this trigger point we recalculate the peak events, or cutting points, used in the computeMeanwave algorithm:

$$\text{events} = \text{events} + \text{trigger} - \text{winsize}/2 \quad (4)$$

With the events variable recalculated, we used the computeMeanWave function again, so the cycles were aligned and the resultant *mean wave* more accurate.

3.2 Clustering

Algorithm 5	distanceMatrix
Input:	Signal, Cutting events, window size.
Output:	Matrix with wave-to-wave distances.

For the clustering procedure we developed a function that receives the signal to cluster, the window size and cutting events produced with the autoMeanwave algorithm.

We go through all the cutting events and for each we select a part of the signal with center at that event and a number of samples to both sizes equal to the window size. Then we compare that cut with each of the others (with the center in the others cutting events and the same window size), using the distance wave-to-wave formula:

$$f(x) = \sqrt{\sum \left(\frac{s_1 - \text{mean}(s_1)}{\text{std}(s_1)} - \frac{s_2 - \text{mean}(s_2)}{\text{std}(s_2)} \right)^2} \quad (5)$$

With s_1 and s_2 being the parts of the signal selected before.

With all of the distance values for each wave, we built a matrix of distances.

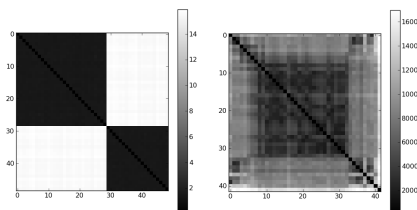


Figure 9: Matrix of distances produced for the synthetic waves (a) and the skiing task (b).

Figure 9 presents two matrixes of distances, obtained with the `imshow` command. Figure 9 a) shows the matrix of the synthetic waves distances and figure 9 b) the matrix for the skiing task distances. As we can see, the synthetic matrix is almost ideal, as all the waves are equal – the distance values only are minimums or maximums. In the skiing matrix however, the matrix assumes a greater variation of distances, as the cycles are not exactly the same. However, it's visible the similarity between the cycles of the same technique (7 cycles V2, 27 cycles V1 and 8 cycles V2).

To cluster the signal we used the `kmeans` algorithm. Those functions received the matrix created with the `distanceMatrix` algorithm and

the number of clusters expected in the data, giving the clusters and distances to the clusters as result.

4 RESULTS AND DISCUSSION

Figure 10 shows the graphics of the resulting *mean waves* (line) and deviation error area (filling) after running the algorithms referenced above. At the left (figure 10 a.) the graphics represent the initial *mean waves* created, before the clustering procedure. At the right (figure 10 b.) we have the *mean waves* representative of the signal parts that were divided according to the resultant clustering codebook.

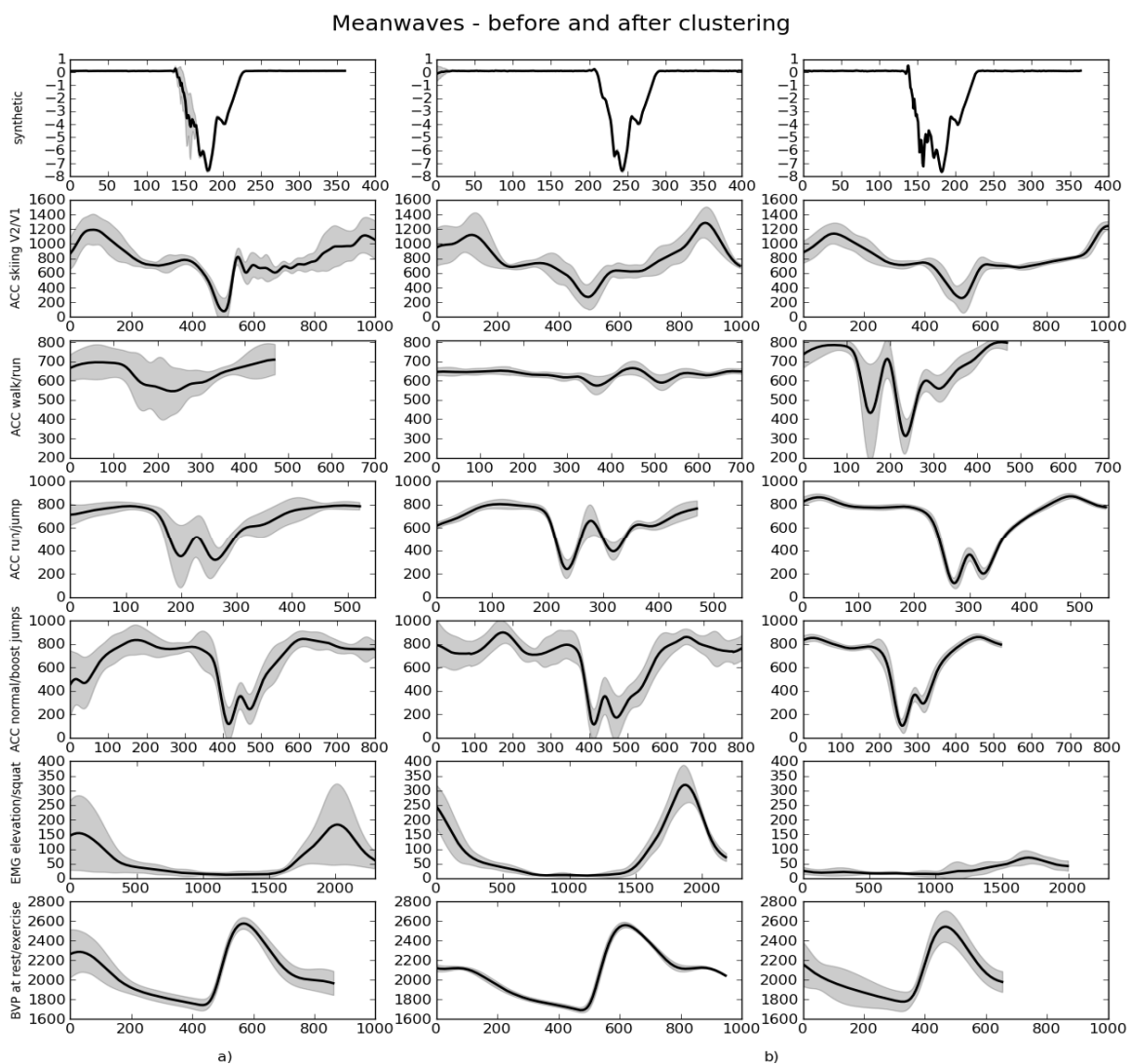


Figure 10: *Mean waves* of all the tasks before (a) and after (b) the clustering procedure.

It's visible that the *mean waves* at the left gather information about the behavior of the signal, even if there are some changes in shape or frequency along the signal. After the clustering procedure there are some predictable variations in the resultant *mean waves*. We notice an overall reduction of the deviation error after the clustering procedure and also a reshaping of the *mean wave*.

After running the clustering procedure we gather the results for each task performed. These results are shown in table 1.

Table 1: Clustering results

Task	Number of Cycles	Cycles correctly clustered	Errors	Misses
Synthetic	50	49	0	1
Walk and run	343	342	1	0
Run and jump	296	295	1	0
Jumps	85	84	1	0
Skiing	42	41	0	1
Elevation and squat	23	23	0	0
BVP rest and after exercise	165	159	4	2
All	1004	991	7	5

It is important to note that some cycles weren't classified, and that occurred because sometimes the borders of the signal didn't have a full cycle - the `distanceMatrix` algorithm (algorithm 5) cannot be used to compare a short cycle with the regular ones. Therefore, those cycles have been rejected for lack of pattern quality, and won't be taken into account.

In the "walk and run" activity there were some extra classification points. The cycles were correctly clustered (with only 1 error encountered), but in the "walking" mode there were some extra points between those cycles that were also classified. The reason is a relatively large variation in the fundamental frequency from the walking to the running activity - despite one activity has all cycles well defined (by events variable described at (4)), the other as less than one cycle per period cut (because of that change of fundamental frequency). This condition shows a limitation of our algorithm - doesn't allow big changes in the frequency domain in the different modes presented on the signal.

The errors of classification, note that only 7 errors were encountered, and 2 of those errors were in transition periods - where the cycle wave is still reshaping to form the other activity and the distance value to the *mean wave* or to the clusters mean values is bigger than anywhere else on the signal. This occurred in the jumps and in the walk and run activities.

Given the results we can affirm that our clustering algorithm based on the *mean wave* information only returned 7 errors out of 999 cycles with pattern quality, and therefore we achieved 99.2% of efficiency.

5 CONCLUSIONS

The proposed algorithm represents an advance in the abstract clustering area, as it has an effective detection of signal variations, tracing different patterns for distinct clusters, whether it's an activity, synthetic or physiological signal.

FUTURE WORK

In future work we intend to repeat this procedure to a wide range of subjects performing the same task, perform a noise immunity test and also run the algorithm using a signal with more than two modes.

We intend to introduce an automatically perception of the cycles which are too distance from the cluster and assign those cycles to a new "rejection class". This will reduce the number of errors due to a strange cycle, in particular the mode's transition cycles.

The local detection of the fundamental frequency is also a future goal, as we intend to realize when there's a major variation of fundamental frequency and make our algorithms adapt its behavior according to that variation.

Finally, we have the intention of creating a multimodal algorithm, which can receive more than one signal, and process those at the same time and with the same treatment. This could be useful if we want to use the 3 axis of an accelerometer, or conciliate the information of a BVP with an electrocardiography (ECG) signal.

ACKNOWLEDGEMENTS

The authors would like to thank PLUX – Wireless Biosignals for providing the acquisition system and sensors necessary to this investigation. We also like to thank NIH, the Norwegian School of Sports and Science, Håvard Myklebust and Jostein Hallén for acquiring and allowing us to work with the Skiing signal used in this study. We acknowledge Rui Martins and José Medeiros for their help and advices on the BVP acquisition procedure.

Information Systems, 14:1–37. DOI 10.1007/s10115-007-0114-2
www.opensignals.net, last accessed on 15/07/2010

REFERENCES

- Andersson, E., Supej, M., Sandbakk, Ø., Sperlich, B., Stöggl, T., Holmberg, H. (2010) Analysis of sprint cross-country skiing using a differential global navigation satellite system. *Eur J Appl Physiol*. DOI 10.1007/s00421-010-1535-2
- Baek, J., Lee G., Park, W., Yun, B. (2004). Accelerometer Signal Processing for User Activity Detection, *Knowledge-Based Intelligent Information & Engineering Systems*, Vol. 3215/2004, 610-617. DOI 10.1007/978-3-540-30134-9_82
- Ben-Arie, J., Wang, Z., Pandit, P., Rajaram, S. (2002). Human Activity Recognition Using Multidimensional Indexing. *IEEE Transactions on Pattern Analysis and Machine Intelligence*, vol. 24, no. 8, 1091-1104.
- Fridlund, A., Schwartz, G., Fowler, S. (2007) Pattern Recognition of Self-Reported Emotional State from Multiple-Site Facial EMG Activity During Affective Imagery. *Society for Psychophysiological Research.*, vol. 21, no. 6. DOI 10.1111/j.1469-8986.1984.tb00249.x
- Liao, T. Warren. (2005) Clustering of time series data – a survey. *Pattern Recognition* 38 (2005) 1857 – 1874.
- Martins, D., Mattos, M., Simões, P., Cechinel, C., Bettiol, J.; Barbosa, A. (2008) Aplicação do Algoritmo K-Means em Dados de Prevalência da Asma e Rinite em Escolares. In: *XI Congresso Brasileiro de Informática em Saúde (CBIS'2008)*, 2008.
- PLUX – Wireless Biosignals, bioPLUX Research Manual, PLUX's internal report, 2010.
- Quiroga, Rodrigo Q. (2007) Spike sorting. *Scholarpedia*, 2(12):3583
- Smith, J., Fishkin, K., Jiang, B., Mamishev, A., Philipose, M., Rea, A., Roy, S., Sundara-Rajan, K. (2005). RFID-Based Techniques for Human-Activity Detection. *Communications of the ACM*, vol. 48, no. 9, 39-44.
- T. Oliphant. Guide to Numpy. Tregol Publishing, 2006.
- T. Oliphant. SciPy Tutorial. SciPy, [http://www.scipy.org/SciPy Tutorial](http://www.scipy.org/SciPy%20Tutorial), 2007.
- Wu, X., Kumar, V., Quinlan J., Ghosh J., Yang, Q., Motoda, H., McLachlan, G., Ng, A., Liu, B., Yu, P., Zhou, Z., Steinbach, M., Hand, D., Steinberg, D. (2007). Top 10 algorithms in data mining. *Knowledge*